

# Electrochemical and Spectroscopic Studies of 3,5-Di-*tert*-butyl-2-aminophenol and of Electrosynthesized 3,5-Di-*tert*-butyl-2-iminocyclohexa-3,5-dienone in Aprotic Solvents

Subhash P. Harmalker and Donald T. Sawyer\*

Department of Chemistry, University of California, Riverside, California 92521

Received January 24, 1984

In acetonitrile 3,5-di-*tert*-butyl-2-iminocyclohexa-3,5-dienone (DTBQI) is the major product from the controlled-potential electrooxidation of 3,5-di-*tert*-butyl-2-aminophenol (DTBAPH<sub>2</sub>). The same product results from the chemical oxidation of DTBAPH<sub>2</sub> by PbO<sub>2</sub>. The redox chemistry for DTBAPH<sub>2</sub>, DTBQI, and *o*-aminophenol in dimethyl sulfoxide and acetonitrile has been studied with cyclic voltammetry and controlled-potential electrolysis, and the products and intermediates have been characterized by <sup>1</sup>H and <sup>13</sup>C NMR, ESR, IR, and UV-vis spectroscopy. Addition of strong base (OH<sup>-</sup>) to DTBQI causes it to be reduced to a product with the characteristics of DTBAPH<sup>-</sup>. Redox reaction mechanisms are proposed for the electrochemical oxidation of DTBAPH<sup>-</sup> to DTBQI and for the latter's reduction.

A long-standing interest<sup>1</sup> in the catecholate complexes of metal ions prompted the consideration of *o*-aminophenol as an alternative ligand for the stabilization of the manganese(III) ion.<sup>2</sup> As with the catechols,<sup>3</sup> *o*-aminophenol is redox active and its oxidation products are subject to condensation reactions. Hence, a systematic study of the *o*-aminophenol complexes of manganese ions (and their redox chemistry) requires a prior understanding of the redox chemistry of the ligand and its oxidation product, *o*-benzoquinone imine. Because the redox chemistry of *o*-aminophenol is complicated by intermolecular reactions and hydrolysis of the intermediates, derivatives with protective groups provide a useful means to overcome such problems.

The present paper summarizes (a) the results of an electrochemical and spectroscopic study of 3,5-di-*tert*-butyl-2-aminophenol and *o*-aminophenol and (b) the synthesis and characterization of 3,5-di-*tert*-butyl-2-iminocyclohexa-3,5-dienone.

The mechanisms of formation for quinone imine dyes have been discussed in a recent paper.<sup>4</sup> Earlier studies<sup>5,6</sup> confirm that benzoquinone imines are extremely unstable compounds and are subject to rapid hydrolysis. The latter process has been studied by cyclic voltammetry.<sup>7</sup> Studies of quinone imine chemistry have been facilitated by its *in situ* generation.<sup>4,6</sup>

## Experimental Section

**Equipment.** The cyclic voltammetry and controlled-potential electrolyses were performed with a three-electrode potentiostat (Princeton Applied Research Model 173 Potentiostat/Galvanostat, Model 175 Universal Programmer and Model 179 Digital Coulometer) and a Houston Instruments Model 100 Omnigraphic X-Y recorder. The electrochemical measurements were made with a two-compartment cell that was bridged by a 10-cm-long double-fritted horizontal Pyrex tube; the latter was filled with supporting electrolyte solution. The working electrode compartment contained a Beckman platinum inlay working electrode (area, 0.23 cm<sup>2</sup>) and an Ag/AgCl, cracked-glass bead, reference electrode

(filled with aqueous tetramethylammonium chloride solution and adjusted to 0.000 V vs. SCE) in a luggin capillary. The auxiliary compartment contained a platinum flag electrode. Platinum mesh working and auxiliary electrodes were used for the controlled-potential electrolyses. All of the work was carried out in a Vacuum Atmosphere glovebox (dry N<sub>2</sub> atmosphere).

The UV-vis spectrophotometric measurements were made with Cary Model 17D and 219 spectrophotometers, the EPR spectra were recorded with a Bruker ER200D EPR spectrometer, and the <sup>13</sup>C and <sup>1</sup>H NMR spectra were obtained with either a JEOL JNM-FX200 or a Nicolet NIC-300 FT-NMR spectrometer. The IR spectra were recorded with a Perkin-Elmer Model 283 infrared spectrophotometer.

**Reagents.** The chemicals for the syntheses and electrochemical experiments included 3,5-di-*tert*-butylphenol (Aldrich), sodium hydrosulfite (Mallinckrodt), sodium hydroxide (Mallinckrodt), lead dioxide (Mallinckrodt), tetraethylammonium hydroxide (TEAOH, 25% in methanol) (Eastman Kodak Company), tetraethylammonium perchlorate (TEAP) (G. Frederick Smith), and ethyl alcohol (Goldshield Chemical Company). The solvents for the electrochemical measurements (acetonitrile, dimethyl sulfoxide, and pyridine) were supplied by Burdick and Jackson Laboratories ("distilled in glass" grade) with water contents of <0.01%.

**3,5-Di-*tert*-butyl-2-aminophenol (DTBAPH<sub>2</sub>).** This compound was prepared by a modified version of a published procedure.<sup>8</sup> A solution of synthesized<sup>9</sup> 2-nitro-3,5-di-*tert*-butylphenol (10 g, 0.04 mol) in 20 mL of ethanol was made alkaline with NaOH (2 g in 20 mL of H<sub>2</sub>O) and then treated dropwise with a solution of NaHSO<sub>3</sub> [28 g in 100 mL of H<sub>2</sub>O (twice the amount used in the published procedure)<sup>8</sup>] at room temperature under an argon atmosphere over a period of 20 min. The acidity of the solution was controlled at pH 11.00 by the simultaneous addition of base (10 g of NaOH in 100 mL of H<sub>2</sub>O). After the solution had stirred overnight under an argon atmosphere, it was diluted to 1.6 L by being poured into water and then acidified with dilute HCl to give a yellowish white precipitate. The latter was isolated, washed with *n*-hexane, and recrystallized from hot *n*-heptane to yield a fibrous white solid (mp 167 °C; IR 3323 cm<sup>-1</sup> and 3422 cm<sup>-1</sup> (N-H) and 3180 cm<sup>-1</sup> (O-H)). The melting point and the IR bands are consistent with those in the literature.<sup>5</sup>

**3,5-Di-*tert*-butyl-2-iminocyclohexa-3,5-dienone (DTBQI).** A solution of DTBAPH<sub>2</sub> (100 mg in 50 mL of acetonitrile) was stirred with excess lead dioxide (5 g) for 12 h under an argon atmosphere at room temperature. It was then filtered, and the filtrate was evaporated to dryness with a rotary evaporator at room temperature to give a yellow product (mp 64 °C; 100% yield). (The concentration of DTBAPH<sub>2</sub> was critical; at higher concentrations and temperatures the product hydrolyzed to 3,5-di-*tert*-butyl-*o*-benzoquinone and turned brown.) (Galbraith Laboratories). Calcd for C<sub>14</sub>H<sub>21</sub>NO: C, 76.70; H, 9.59; N, 6.39; O, 7.30.

(1) Chin, D.-H.; Jones, S. E.; Leon, L. E.; Bosserman, P.; Stallings, M. D.; Sawyer, D. T. *Adv. Chem. Ser.* 1982, 201, 675.

(2) Chin, D.-H.; Sawyer, D. T.; Schaefer, W. P.; Simmons, C. J. *Inorg. Chem.* 1983, 22, 752.

(3) Stallings, M. D.; Morrison, M. M.; Sawyer, D. T. *Inorg. Chem.* 1981, 20, 2655.

(4) Brown, K. C.; Corbett, J. F. *J. Chem. Soc., Perkin Trans. 2* 1979, 304; *Ibid.* 1981, 886, and references therein.

(5) Patai, S., Ed. "Chemistry of Carbon-Nitrogen Double Bond"; Interscience: New York, 1970.

(6) Nogani, T.; Hishida, T.; Yamada, M.; Mikawa, H.; Shiota, Y. *Bull. Chem. Soc. Jpn.* 1975, 48, 3709.

(7) Adams, R. N. "Electrochemistry at Solid Electrodes"; Marcel Dekker: New York, 1969; pp 336-345.

(8) Okazaki, R.; Hosogai, T.; Hashimoto, M.; Inamoto, N. *Bull. Chem. Soc. Jpn.* 1969, 42, 3559.

(9) Elder, J. W.; Mariella, P. *Can. J. Chem.* 1963, 41, 1653.

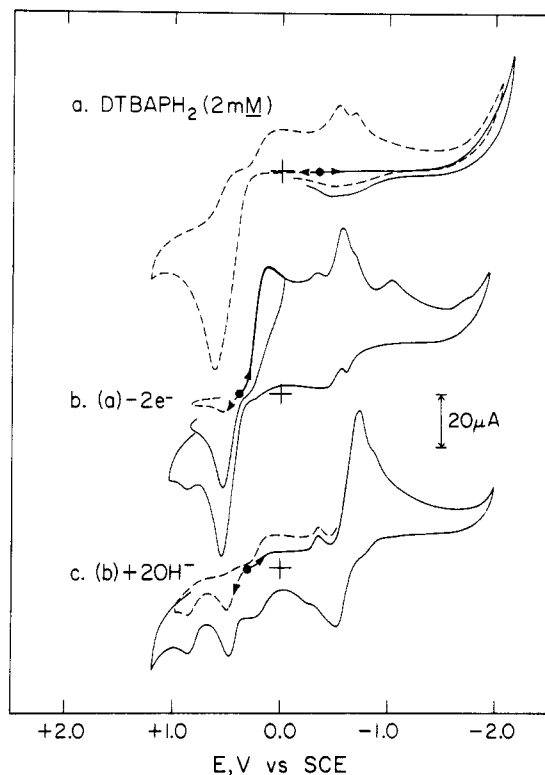


**Figure 1.** Cyclic voltammograms in  $\text{Me}_2\text{SO}$  (0.1 M TEAP) of (a)  $\text{DTBAPH}_2$ , (b) the product from the two-electron oxidation of  $\text{DTBAPH}_2$  at +0.6 V vs. SCE, and (c) solution (b) after the addition of 2 equiv of  $\text{OH}^-$ . Platinum electrode, area  $0.23 \text{ cm}^2$ ; scan rate,  $0.1 \text{ V s}^{-1}$ .

Found: C, 76.74; H, 9.46; N, 6.49; O, 7.43. IR:  $3200 \text{ cm}^{-1}$  ( $=\text{NH}$ ) and  $1670 \text{ cm}^{-1}$  ( $\text{C}=\text{O}$ ).

The same product (DTBQI) was prepared by electrochemical oxidation at  $-0.30 \text{ V}$  vs. SCE of 20 mM (0.22 g)  $\text{DTBAPH}_2$  in  $\text{MeCN}$  (50 mL; 0.1 M TEAP) that contained 20 mM tetraethylammonium hydroxide (TEAOH) under a nitrogen atmosphere. The electrolysis removed approximately  $1 \text{ e}^-/\text{DTBAPH}_2$  and the solution turned yellow. It was evaporated to dryness under vacuum at room temperature to yield a yellow solid, which was dissolved in *n*-hexane (the TEAP remained undissolved). The yellow solution was filtered and the filtrate evaporated to dryness. Next, the residue was treated with cold *n*-heptane; a white solid ( $\text{DTBAPH}_2$ ) remained undissolved and was removed by filtration. The yellow filtrate was evaporated to dryness to give a yellow solid (mp  $65^\circ \text{C}$ ; IR  $3200 \text{ cm}^{-1}$  ( $=\text{NH}$ ) and  $1670 \text{ cm}^{-1}$  ( $\text{C}=\text{O}$ )). This compound exhibited the same  $^{13}\text{C}$  and  $^1\text{H}$  NMR spectra and electrochemistry as chemically synthesized DTBQI.

Electrochemical oxidation at +0.9 V vs. SCE of neutral 20 mM (0.22 g)  $\text{DTBAPH}_2$  in  $\text{Me}_2\text{SO}$  (50 mL, 0.1 M TEAP) removed  $2 \text{ e}^-/\text{DTBAPH}_2$  to give a yellow solution which turned red at the end of the electrolysis. When the solution was evaporated under vacuum at  $\sim 50^\circ \text{C}$ , it turned red-brown and a yellow liquid distilled over into the trap (probably DTBQI, mp  $65^\circ \text{C}$ ). The residue was dissolved in *n*-heptane to remove TEAP, the filtrate evaporated to dryness, and the precipitate recrystallized from *n*-heptane to yield a brown solid. IR and  $^1\text{H}$  NMR spectroscopic data for the product were identical with those for 3,5-di-*tert*-butyl-*o*-benzoquinone (DTBQ).

## Results

**Electrochemistry.** Figure 1a illustrates the cyclic voltammograms for 3,5-di-*tert*-butyl-2-aminophenol ( $\text{DTBAPH}_2$ ) in dimethyl sulfoxide ( $\text{Me}_2\text{SO}$ ). The broad, irreversible oxidation at +0.60 V vs. SCE represents a two-electron process on the basis of controlled-potential coulometric electrolysis. The yellow product solution from such an electrooxidation exhibits a well-defined cyclic voltammogram (Figure 1b;  $E_{\text{pc}}$ , +0.12 V,  $-0.35 \text{ V}$ ,  $-0.6 \text{ V}$ ,

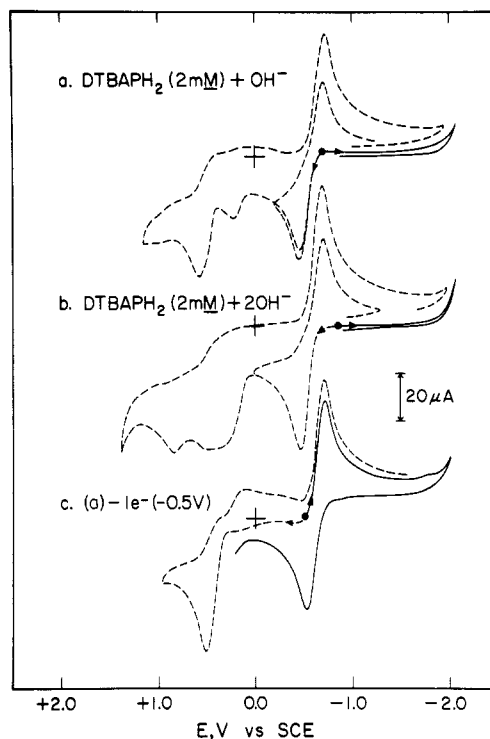


**Figure 2.** Cyclic voltammograms in  $\text{Me}_2\text{SO}$  (0.1 M TEAP) of (a)  $\text{DTBAPH}^-$ , (b)  $\text{DTBAPH}^-$  plus 1 equiv of  $\text{OH}^-$ , and (c) the product from the one-electron oxidation of solution (a) at  $-0.5 \text{ V}$  vs. SCE. Platinum electrode, area  $0.23 \text{ cm}^2$ ; scan rate,  $0.1 \text{ V s}^{-1}$ .

$-0.7 \text{ V}$ ,  $-1.05 \text{ V}$ , and  $-1.6 \text{ V}$  vs. SCE). The reverse scan of an initial negative scan has anodic peaks at  $-0.62 \text{ V}$ ,  $-0.45 \text{ V}$ ,  $+0.55 \text{ V}$ , and  $+0.85 \text{ V}$  vs. SCE. Addition of 2 equiv of  $\text{OH}^-$  to this solution causes the cathodic peak at  $+0.12 \text{ V}$  to shift to  $-0.72 \text{ V}$  (Figure 1c); the latter is coupled to an anodic peak at  $-0.5 \text{ V}$ .

The cyclic voltammograms for  $\text{DTBAPH}_2$  in the presence of 1 and 2 equiv of base and for its oxidation product in the presence of 1 equiv of base are shown in Figure 2. The first of the two major anodic peaks ( $-0.5 \text{ V}$  and  $+0.5 \text{ V}$ ) for  $\text{DTBAPH}^-$  is coupled to a cathodic peak at  $-0.7 \text{ V}$  (Figure 2b). Addition of a second equivalent of base does not change the current of the anodic peak at  $-0.5 \text{ V}$  (Figure 2b), but a broad peak appears at  $\sim +0.3 \text{ V}$  as well as a peak at  $+0.8 \text{ V}$  (the latter corresponds to the oxidation of  $\text{OH}^-$ ).

Controlled-potential oxidation of  $\text{DTBAPH}^-$  at  $-0.5 \text{ V}$  removes  $\sim 1 \text{ e}^-/\text{DTBAPH}^-$  to give a yellow product solution. The cyclic voltammogram for the latter (Figure 2c) has a cathodic peak at  $-0.73 \text{ V}$  for an initial negative scan, which is coupled to an anodic peak at  $-0.5 \text{ V}$ . An initial positive scan yields an anodic peak at  $+0.5 \text{ V}$  that corresponds to a 50% yield of  $\text{DTBAPH}_2$  from the electrolysis. Controlled-potential oxidation of this solution at  $+0.5 \text{ V}$  removes  $\sim 1 \text{ e}^-/\text{DTBAPH}_2$ .

In acetonitrile ( $\text{MeCN}$ ),  $\text{DTBAPH}_2$  exhibits an anodic peak at  $+0.6 \text{ V}$  for an initial positive scan and a cathodic peak at  $-1.5 \text{ V}$  for an initial negative scan. Controlled-potential oxidation at  $+0.6 \text{ V}$  removes  $1 \text{ e}^-/\text{DTBAPH}_2$  and results in a yellow solution, which exhibits a cyclic voltammogram that is characteristic of 3,5-di-*tert*-butyl-2-iminocyclohexa-3,5-dienone (DTBQI) and an absorption band at  $390 \text{ nm}$  that is equivalent to that for an approximate 40% yield of DTBQI.

The cyclic voltammogram for *o*-aminophenol (OAP) in  $\text{MeCN}$  and its one-electron oxidation product are shown in Figure 3). Controlled-potential oxidation of OAP at  $+1.0 \text{ V}$  removes one electron per OAP to yield a car-

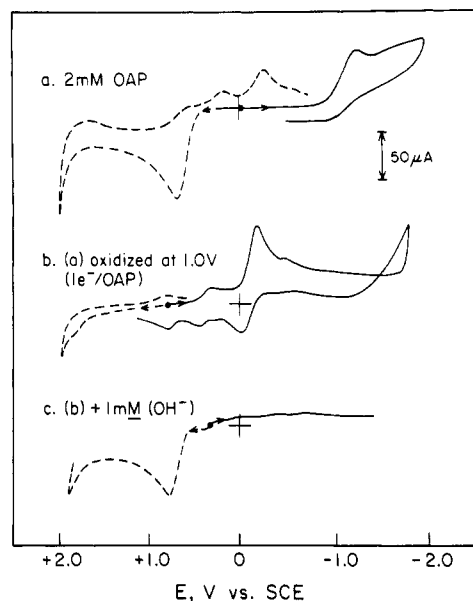


**Figure 3.** Cyclic voltammograms in MeCN (0.1 M TEAP) of (a) *o*-aminophenol (OAP), (b) the product from the one-electron oxidation of OAP, and (c) solution (b) after the addition of 0.5 equiv of  $\text{OH}^-$ . Platinum electrode, area  $0.23 \text{ cm}^2$ ; scan rate,  $0.1 \text{ V s}^{-1}$ .

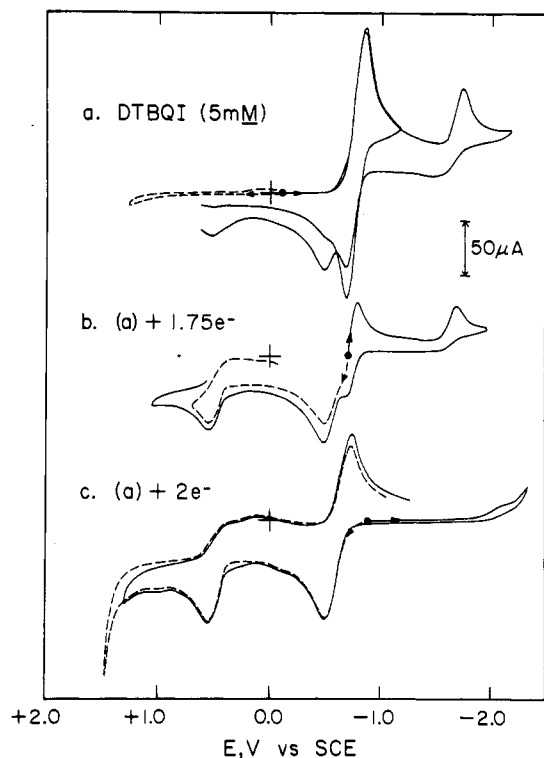


**Figure 4.** Cyclic voltammograms in  $\text{Me}_2\text{SO}$  (0.1 M TEAP) of (a) DTBQI, (b) the product from the 1.75-electron reduction of DTBQI, and (c) the product from the two-electron reduction of DTBQI. Platinum electrode, area  $0.23 \text{ cm}^2$ ; scan rate,  $0.1 \text{ V s}^{-1}$ .

mine-red solution. The latter has a major reduction peak at  $-0.2 \text{ V}$  (Figure 3b) that is similar to the one for protonated *o*-aminophenol (1:1  $\text{HClO}_4$ :OAP). Addition of one-half of an equivalent of  $\text{OH}^-$  to the carmine-red solution yields a yellow solution and eliminates the  $-0.2\text{-V}$  reduction peak (Figure 3c); the cyclic voltammogram has an anodic peak at  $+0.8 \text{ V}$  that corresponds to a 75% yield of OAP.

Figure 4 illustrates the cyclic voltammograms for 3,5-di-*tert*-butyl-2-iminocyclohexa-3,5-dienone (DTBQI)

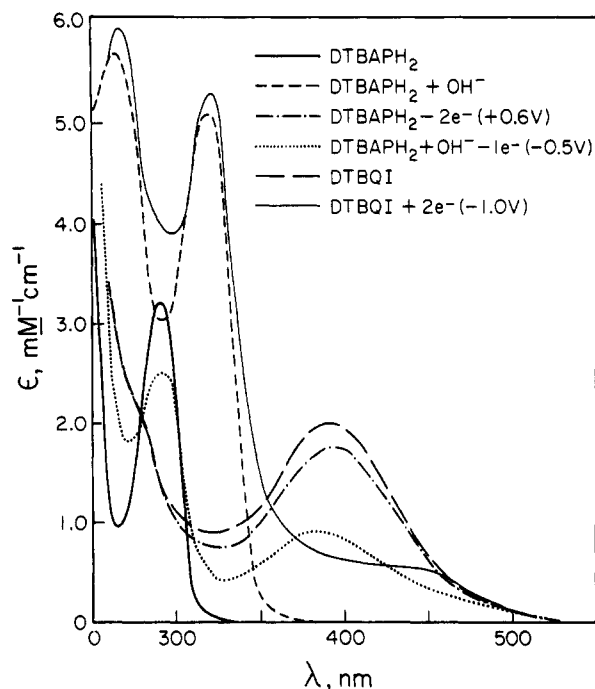


**Figure 5.** Absorption spectra in  $\text{Me}_2\text{SO}$  (0.1 M TEAP) of DTBAPH<sub>2</sub>, DTBAPH<sup>-</sup>, the two-electron oxidation product from electrolysis of DTBAPH<sub>2</sub>, the one-electron oxidation product from electrolysis of DTBAPH<sup>-</sup>, DTBQI, and the two-electron reduction product from electrolysis of DTBQI.

**Table I.** UV-Vis Absorption Bands for DTBAPH<sub>2</sub>, DTBAPH<sup>-</sup>, DTBQI, and Their Redox Products in  $\text{Me}_2\text{SO}$  (0.1 M TEAP)

compound	$\lambda_{\text{nm}}$ ( $\epsilon$ , $\text{M}^{-1} \text{ cm}^{-1}$ )
DTBAPH <sub>2</sub>	290 (3200)
DTBAPH <sub>2</sub> - 2 e <sup>-</sup> (+0.6 V vs. SCE)	390 (1700)
DTBAPH <sup>-</sup>	315 (5100), 265 (5700)
DTBAPH <sup>-</sup> - e <sup>-</sup> (-0.5 V)	385 (900), 290 (2500)
DTBQI (from chemical synthesis)	390 (2000)
QI + 2 e <sup>-</sup> (-1.0 V)	325 (5200), 270 (6000)

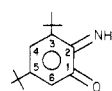
(prepared by  $\text{PhO}_2$  oxidation of DTBAPH<sub>2</sub>) and its reduction products. The presence of water in the solvent causes the cathodic peak at  $-0.85 \text{ V}$  to be shifted to more negative potentials and to increase in height at the expense of the peak at  $-1.75 \text{ V}$ .

When solutions of DTBQI are reduced by controlled-potential electrolysis at  $-1.0 \text{ V}$ , they initially turn green and then become yellow. The cyclic voltammogram of the electrolyzed solution (after passing  $1.75 \text{ e}^-/\text{DTBQI}$ ) exhibits a small anodic shoulder at  $-0.7 \text{ V}$  (Figure 4b). The complete reduction of DTBQI consumes  $2 \text{ e}^-/\text{DTBQI}$  to give a product solution with a cyclic voltammogram (Figure 4c) that is identical with that for a 1:1 DTBAPH<sub>2</sub>: $\text{OH}^-$  solution (Figure 2a). The green intermediate species is stabilized by the use of a pyridine solvent system for the electrochemical reduction of DTBQI. Addition of an equivalent of  $\text{OH}^-$  to a solution of DTBQI in  $\text{Me}_2\text{SO}$  causes a transient green color before the solution rapidly becomes pale yellow. The cyclic voltammogram of the latter solution is identical with that for the two-electron reduction product of DTBQI (Figure 4c).

**Optical Spectroscopy.** The UV-vis spectra for DTBQI, DTBAPH<sub>2</sub>, DTBAPH<sup>-</sup>, and their redox products are shown in Figure 5, and the absorption bands for the various compounds and intermediates are listed in Table I. The two-electron reduction product of DTBQI exhibits a spectrum similar to that for DTBAPH<sup>-</sup>, and the product

**Table II.**  $^1\text{H}$  and  $^{13}\text{C}$  NMR Data for DTBQI<sup>a</sup> and 3,5-Di-*tert*-butyl-*o*-benzoquinone (DTBQ)

C position <sup>a</sup>	DTBQI <sup>b</sup>	DTBQ <sup>b</sup>
A. $^1\text{H}$ Chemical Shifts in $\text{CD}_3\text{CN}$ vs. $\text{Me}_4\text{Si}$ , ppm		
6- <i>t</i> -Bu	6.72 (t)	7.02 (d)
4- <i>t</i> -Bu	6.18 (d)	6.13 (d)
3	1.37 (s)	1.23 (s)
5	1.20 (s)	1.20 (s)
B. $^{13}\text{C}$ (H Decoupled) Chemical Shifts in $\text{CDCl}_3$ vs. $\text{Me}_4\text{Si}$ , ppm		
1	179.4	179.9
2	166.1	180.9
4, 6	162.3, 151.7	163.1, 149.8
5, 3	126.2, 120.3	133.3, 121.9
5-, 3- <i>t</i> -Bu	36.6, 35.3	35.8, 35.3
(Me) <sub>3</sub> [5,3- <i>t</i> -Bu]	30.2, 28.2	29.1, 27.7

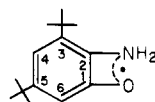
<sup>a</sup><sup>b</sup> t, triplet; d, doublet; s, singlet.

from the two-electron oxidation of DTBAPH<sub>2</sub> in Me<sub>2</sub>SO has a unique band at 390 nm ( $\epsilon$  1700 M<sup>-1</sup> cm<sup>-1</sup>) and a shoulder at 280 nm (Figure 5). The product from the one-electron oxidation of DTBAPH<sup>-</sup> has a spectrum that is closely similar to that for a 1:1 mixture of DTBQI and DTBAPH<sub>2</sub>. Further oxidation of such a solution causes the DTBQI band (385 nm) to increase in intensity at the expense of the DTBAPH<sub>2</sub> band (290 nm).

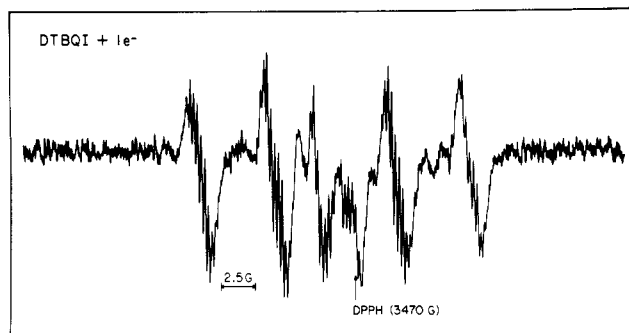
The UV-vis spectrum for DTBQI in the presence of an equivalent of OH<sup>-</sup> (TEAOH in methanol) in Me<sub>2</sub>SO is identical with that for the two-electron reduction product of DTBQI (Figure 5), except at 90% in intensity. The apparent second-order rate constant ( $k_2$ ) for the DTBQI + OH<sup>-</sup> reaction is about 20 M<sup>-1</sup> s<sup>-1</sup> (on the basis of the decay rate for the DTBQI absorbance at 390 nm).

**$^1\text{H}$  NMR and  $^{13}\text{C}$  (Proton Decoupled) NMR.** The  $^1\text{H}$  NMR and  $^{13}\text{C}$  NMR data for DTBQI and DTBQ (for comparison) are summarized in Table II. Both exhibit six  $^{13}\text{C}$  resonances in the aromatic region, and one of the carbonyl carbon resonances of DTBQ (180.9 ppm) shifts to higher field (166.1 ppm) in DTBQI. The NMR spectra for DTBQI in Me<sub>2</sub>SO-*d*<sub>6</sub> to which an equivalent of OH<sup>-</sup> (TEAOH) has been added [ $^1\text{H}$  NMR 6.2 (d), 6.0 (d);  $^{13}\text{C}$  (proton decoupled) NMR 158.6, 138.4, 133.2, 110.4, 103.7] are identical in the aromatic region with those for DTBAPH<sup>-</sup> in Me<sub>2</sub>SO-*d*<sub>6</sub>.

**ESR Spectrum.** The ESR spectrum for DTBQI that has been reduced by one-electron (Figure 6) exhibits five major lines (with the central line split into a doublet); the coupling constant is about 5 G. The five lines appear to have almost equal intensities with each one split into about 15 lines (coupling constant, 0.25 G). The spectrum of Figure 6 can be simulated by assuming  $A_N = 5$  G,  $A_{H_N} = 5$  G,  $A_{H_6} = 0.5$  G, and  $A_{H(3-t-Bu,3)} = 0.25$  G for the neutral radical (DTBQIH $\cdot$ ).

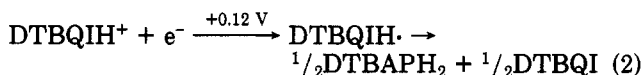


However, the line intensities for the major lines in the simulated spectrum have intensity ratios of 1:3:4:3:1. Because the half-life for the DTBQI $\cdot$  radical is less than 30 s, reliable relative line intensities could not be recorded. The green solution that results from the addition of an equivalent of OH<sup>-</sup> to DTBQI exhibits the same ESR spectrum (a superhyperfine splitting of  $\sim 0.25$  G and  $g_{av} = 2.0037$ ) as that of Figure 6.

**Figure 6.** ESR spectrum for the reduction product from the one-electron electrolysis at -0.9 V vs. SCE of DTBQI in Me<sub>2</sub>SO (0.1 M TEAP). Data collected at 25 °C.

## Discussion and Conclusions

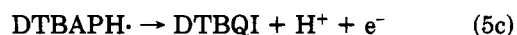
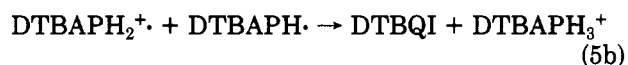
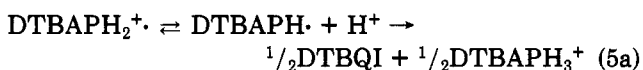
*o*-Aminophenol and *o*-benzoquinone imine represent nitrogen substitution derivatives of catechol and *o*-benzoquinone. These relationships are confirmed by the closely similar electrochemical and spectroscopic properties for DTBAPH<sub>2</sub> and DTBQI when compared with those for their catechol and *o*-benzoquinone analogues.<sup>3</sup> Hence, DTBAPH<sub>2</sub> is electrochemically oxidized to give the protonated form of DTBQI (eq 1), which is reduced (Figure 1b) to a neutral radical that disproportionates (eq 2).



Thus, the reduction of protonated quinone imine results in the formation of 50% starting material, DTBAPH<sub>2</sub>. The cathodic peak at -0.35 V of Figure 1b corresponds to the reduction of a protonated amine (DTBAPH<sub>3</sub><sup>+</sup> in this case). The cathodic peaks at -0.6 V and -1.05 V of Figure 1b are due to the 3,5-di-*tert*-butyl-*o*-benzoquinone (DTBQ) that is formed by the acid hydrolysis of DTBQI (eq 3); such acid-induced deaminations are characteristic of quinone imines.<sup>4,5,10</sup>



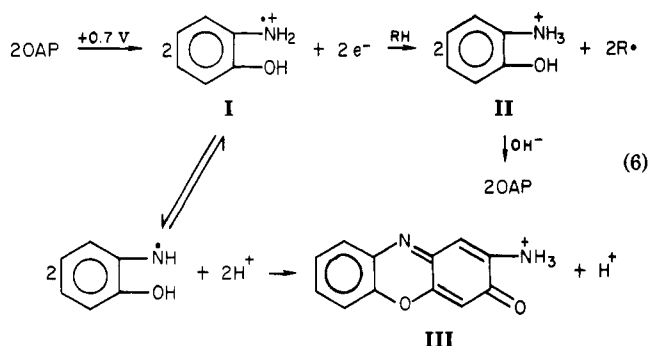
In acetonitrile, DTBAPH<sub>2</sub> is oxidized by a one-electron process to give a 40% yield of DTBQI (on the basis of the electrochemistry and spectroscopy of the product solution) (eq 4 and 5). In MeCN DTBAPH<sub>3</sub><sup>+</sup> is not oxidized, but



the results of Figure 1 indicate that Me<sub>2</sub>SO facilitates its dissociation to give an overall two-electron oxidation of DTBAPH<sub>2</sub>.

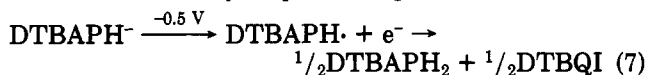
The electrochemical oxidation of unsubstituted *o*-aminophenol (OAP) in MeCN also is a one-electron process. However, instead of a stable quinone imine product, a carmine-red solution results that has similar electrochemistry and  $^1\text{H}$  and  $^{13}\text{C}$  NMR spectra to that of protonated *o*-aminophenol. The carmine-red solution turns yellow upon addition of OH<sup>-</sup> to give neutral OAP. This

reaction sequence is summarized by eq 6. Product I is



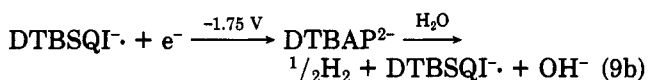
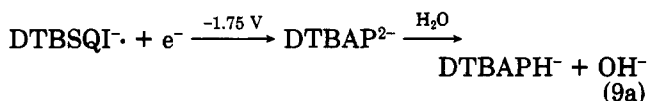
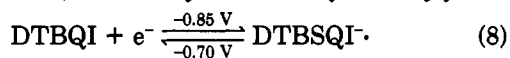
indicated by its ESR spectrum,<sup>11</sup> product II by its electrochemistry and <sup>1</sup>H and <sup>13</sup>C NMR spectra (similar to protonated OAP), and product III by a visible spectrum [ $\lambda$  410 nm ( $\epsilon$  1750 M<sup>-1</sup> cm<sup>-1</sup>) and  $\lambda$  425 nm ( $\epsilon$  1750 M<sup>-1</sup> cm<sup>-1</sup>)] that is similar to that reported in the literature.<sup>6</sup> If the cation radical I undergoes only dissociation and dimerization to III, then removal of one-electron per OAP from two OAP molecules will yield one III. In the case of the oxidation of DTBAPH<sub>2</sub> the ring substitution prevents the formation of products analogous to II and III.

The one-electron oxidation of DTBAPH<sub>2</sub> in the presence of an equivalent of OH<sup>-</sup> results in the formation of 50% DTBQI and 50% DTBAPH<sub>2</sub> (as indicated by spectroscopy and electrochemistry) (eq 7). The product that is isolated



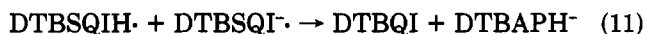
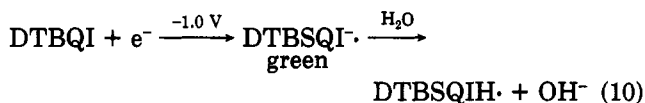
from the electrochemical oxidation of DTBAPH<sup>-</sup> in MeCN is identical with that from the chemical oxidation of DTBAPH<sub>2</sub> by PbO<sub>2</sub>, namely, DTBQI. The <sup>1</sup>H and <sup>13</sup>C NMR chemical shifts (with their assignments) for DTBQI are listed in Table II along with those of DTBQI for comparison.

The electrochemistry of DTBQI is similar to that for DTBQ and can be rationalized by analogous redox reactions<sup>3</sup> (eq 8 and 9). Electrolysis of DTBQI initially yields



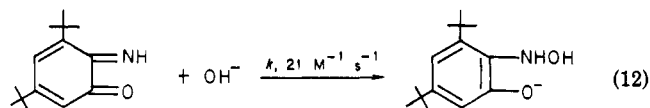
(11) The carmine-red solution (~5% paramagnetic) exhibits an ESR spectrum with seven major lines ( $A_{av} = 4.8$ ,  $g_{av} = 2.0037$ ) with intensity ratios of 1:4:8:10:8:4:1; each of them is split into four lines ( $A_{av} = 1.0$  G).

a green solution that rapidly changes to a pale yellow color. Overall, two electrons are added per DTBQI and the final product solution has the electrochemistry and spectroscopy of DTBAPH<sup>-</sup>. The disproportionation of DTBSQI<sup>•</sup> via hydrolysis and protonation (eq 10 and 11) is consistent



with the increased stability of the green semiquinone imine anion radical in more basic solvents like pyridine. It also accounts for the enhanced height of the first reduction peak for DTBQI in Figure 4 and for the decrease in the height of the second peak upon addition of H<sub>2</sub>O.

The reduction of DTBQI (in Me<sub>2</sub>SO) by addition of an equivalent of OH<sup>-</sup> is confirmed by the electrochemistry and spectroscopy for the product solution; both measurements indicate a species that is equivalent to the DTBAPH<sup>-</sup> anion. A reasonable rationalization for these results is given in eq 12. The <sup>13</sup>C and <sup>1</sup>H NMR spectra for the



product of eq 12 are essentially the same as those for DTBAPH<sup>-</sup>. The transient green color that is observed during the reduction reaction probably is due to the transient formation of a semiquinone imine free radical from oxidation of the monoanion product in eq 12 by DTBQI.

Work in progress is directed to the characterization of the transition-metal (Mn, Fe, and Cu) complexes that are formed by DTBAPH<sup>-</sup> and their redox reactions. Preliminary results indicate that these and other *o*-aminophenol complexes are extremely susceptible to autoxidation and provide an effective means for the activation of dioxygen.

**Acknowledgment.** This work was supported by the National Institutes of Health-USPHS under Grant No. GM22761.

**Registry No.** I, 60715-75-5; II, 63697-25-6; III, 91054-23-8; DTBQI, 91054-21-6; DTBAPH<sub>2</sub>, 24973-57-7; DTBQ, 3383-21-9; OEP, 95-55-6; DTBQIH<sup>•</sup>, 91054-22-7; DTBAPH<sup>-</sup>, 91054-24-9; DTBAPH<sub>2</sub> - 2e<sup>-</sup>, 91054-20-5; DTBQI - 2e<sup>-</sup>, 91054-25-0; PbO<sub>2</sub>, 1309-60-0; 2-nitro-3,5-di-*tert*-butylphenol, 3114-67-8.